J|A|C|S
ARTICLES

Published on Web 06/10/2006

Electronic Properties of Furyl Substituents at Phosphorus and Their Influence on ^{31}P NMR Chemical Shifts

Marco Ackermann,[†] Aurelia Pascariu,[†] Thomas Höcher,[†] Hans-Ullrich Siehl,[‡] and Stefan Berger*[,†]

Contribution from the Institut für Analytische Chemie, Fakultät für Chemie und Mineralogie, Universität Leipzig, Linnéstr. 3, D-04103 Leipzig, Germany and Abteilung für Organische Chemie I, Fakultät für Naturwissenschaften, Universität Ulm, D-89069 Ulm, Germany

Received October 25, 2005; E-mail: stberger@rz.uni-leipzig.de

Abstract: The electronic properties of 2-furyl and 3-furyl substituents attached to phosphanes and phosphonium salts were studied by means of IR spectroscopy and experimental and computational ^{31}P NMR spectroscopy. The heteroaromatic systems proved to be electron withdrawing with respect to phenyl substituents. However, phosphorus atoms with attached furyl substituents are strongly shielded in NMR. The reason for this phenomenon was studied by solid state ^{31}P MAS NMR experiments. The chemical shift tensor was extracted, and the orientation within the molecules was determined. The tensor component σ_{33}, which is effected the most by furyl systems, is oriented perpendicular to the P−C bonds of the substituents. P−furyl bonds are shorter than P−phenyl bonds. We assume therefore a lower ground-state energy of the molecules, because of the electron withdrawing properties of the 2-furyl systems. The σ^{para} component of the ^{31}P NMR magnetic shielding is therefore smaller, which results in an overall increase of the magnetic shielding.

Introduction

In recent years tris(2-furyl)phosphane (TFP) has become an important ligand in transition metal catalysis.[1] TFP was first identified as an exceptional well ligand system for Stille type cross-couplings by Farina et al.[2] This discovery triggered many other investigations concerning the use of TFP in cross-coupling reactions, e.g., in Negishi cross-couplings,[3] Heck reactions,[4] Suzuki reactions,[5] nickel-catalyzed reactions,[6] rhodium-catalyzed reactions,[7] and ruthenium-catalyzed reactions.[8] TFP is highly advantageous especially in Stille type cross-coupling reactions because often a significant rate acceleration is observed over traditional PPh_3 based catalysts. This observation is attributed to the different electronic properties of TFP over PPh_3. TFP is believed to be less Lewis basic and therefore represents a poor σ-donor ligand. In other words, the 2-furyl rings of TFP should be electron withdrawing with respect to phenyl rings, leaving less electron density at the phosphorus nucleus. The furyl substituents of TFP are five-membered aromatic rings with 6 π-electrons and therefore can be regarded as π-excess aromatic systems. From this point of view, electron withdrawing properties of the 2-furyl rings might be surprising. But the oxygen within the ring has a strong −I and a +M effect (Figure 1), which could be responsible for the assumed electron withdrawal of furyl rings.

For 3-furyl systems one could construct similar models; but experimental data are scarce in this case. The −I effect should be smaller since the oxygen phosphorus distance is increased, whereas the +M effect is still present.

However, these ideas are so far only insufficiently verified since the electronic properties of tertiary phosphanes are difficult to quantify. For example, the well-known Tolman angles correlate the steric size of phosphanes with their electronic properties.[9] However the Tolman angle reported for PPh_3 (145°) is only slightly bigger than that for TFP (133°) and therefore does not explain the significant differences in chemical behavior as well as their ligand properties. Another approach to quantifying phosphane basicity was reported by Allen and Taylor.[10] They measured the $^{1}J(^{31}\text{P}-^{77}\text{Se})$ coupling constants of phosphorus selenides. The coupling constant for $Ph_3P{=}Se$ was reported with 732 Hz compared to the TFP based system with 793 Hz. An increase in this coupling constant is attributed to an increased s-character of the phosphorus lone pair. This is the only work reported in the literature, which quantifies the electron withdrawing character of TFP with respect to PPh_3. Many other methods have been suggested to additionally support these findings, including IR stretching frequencies of phosphane transition-metal carbonyl complexes,[11] ^{31}P NMR chemical shift

---

[†] Universität Leipzig.
[‡] Universität Ulm.

(1) Andersen, N. G.; Keay, B. A. *Chem. Rev.* **2001**, *101*, 997.
(2) Farina, V.; Baker, S. R.; Benigni, D. A.; Sapino, C. *Tetrahedron Lett.* **1988**, *29*, 5739.
(3) Klement, I.; Rottländer, M.; Tucker, C. E.; Majid, T. N.; Knochel, P.; Venegas, P.; Cahiez, G. *Tetrahedron* **1996**, *52*, 7201.
(4) Herrmann, W. A.; Brossmer, S.; Öfele, K.; Beller, M.; Fischer, H. *J. Mol. Catal. A: Chem.* **1995**, *103*, 133.
(5) Anderson, J. C.; Namli, H.; Roberts, C. A. *Tetrahedron* **1997**, *53*, 15123.
(6) Shirakawa, E.; Yamasaki, K.; Hiyama, T. *Synthesis* **1998**, 1544.
(7) Sakai, M.; Hayashi, H.; Miyaura, N. *Organometallics* **1997**, *16*, 4229.
(8) Trost, B. M.; Rhee, Y. H. *J. Am. Chem. Soc.* **1999**, *121*, 11680.
(9) (a) Tolman, C. A. *Chem. Rev.* **1977**, *77*, 313. (b) Tolman, C. A. *J. Am. Chem. Soc.* **1970**, *92*, 2953.
(10) Allen, D. W.; Taylor, B. F. *J. Chem. Soc., Dalton Trans.* **1982**, 51.

10.1021/ja057085u CCC: $33.50 © 2006 American Chemical Society

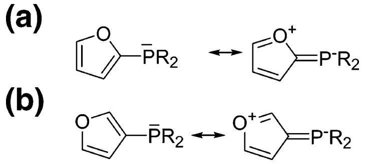

Figure 1. (a) Mesomeric core structures of 2-furyl bearing phosphanes. (b) Mesomeric core structures of 3-furyl bearing phosphanes.

correlation,[12] ${}^1J({}^{31}P-{}^{195}Pt)$ coupling constants,[13] lone pair ionization potential,[14] and gas-phase basicity.[15] However, none of these methods has been applied to TFP or other phosphanes bearing furyl substituents. This work presents some of the lacking experimental data, which should help to understand the electronic properties of TFP. Additionally, the influence of 2-furyl moieties on the ${}^{31}P$ NMR chemical shift will be studied by means of MAS NMR experiments, to extract information about the chemical shift tensor components. Ab initio calculations will clarify the orientation of these tensor components within the molecules, providing an explanation for the observed ${}^{31}P$ NMR chemical shift.

Results and Discussion

Recently we were interested in the use of heteroaromatic substituents at the phosphorus atom of phosphonium salts in Wittig reactions.[16] We prepared (2-furyl)diphenylphosphane **1b**, bis(2-furyl)phenylphosphane **1c**, TFP **1d**, and the corresponding phosphanes bearing 3-furyl groups **1e**−**1g**. These phosphanes were quarternized with ethyliodide yielding the corresponding phosphonium salts **2a**−**2g**. The phosphonium salts were deprotonated using either NaHMDS or *n*-BuLi, and the resulting ylides **3** were reacted with benzaldehyde in Wittig reactions. Figure 2 shows all intermediates during Wittig reactions, which were observed by ${}^{31}P$ NMR spectroscopy.

${}^{31}P$ NMR chemical shift data for the intermediates **1a**−**1g** to **5a**−**5g** are presented in Table 1.

The ${}^{31}P$ NMR resonances of all intermediates are shifted to lower frequencies, when phenyl rings are replaced by 2-furyl or 3-furyl groups. A linear correlation is observed between the number of furyl rings present in the molecule and the extent of the chemical shift movement to lower frequencies. Comparing the influence of 2-furyl and 3-furyl rings on the chemical shift, we conclude that in the case of phosphonium salts and phosphane oxides the 2-furyl rings lead to lower overall chemical shift frequencies (**2d** vs **2g** and **5d** vs **5g**), whereas in the case of phosphanes and oxaphosphetanes the opposite is true (**1d** vs **1g** and **4d** vs **4g**). Overall, the influence of the furyl substituents on the ${}^{31}P$ NMR chemical shift is most pronounced in the phosphanes, since the phosphorus atom in these compounds lacks any other substituents, which could lower the influences of furyl groups.

Lower NMR resonance frequencies as shown in Table 1 correspond to higher shielding. As outlined in the Introduction, furyl substituents attached to phosphorus nuclei are believed to act electron withdrawing, with respect to phenyl rings. The question arose how the postulated electron withdrawing properties of the furyl groups should lead to higher shielded phosphorus nuclei.

Although furyl systems are believed to act electron withdrawing, there is still a considerable lack of experimental data, supporting and quantifying this assumption. Additional data can be obtained from IR investigations.[9,11,12] We therefore prepared carbonyl complexes from the 2-furyl and 3-furyl group bearing phosphanes **1a** to **1g** with $Ni(CO)_4$. From the resulting carbonyl complexes of the general formula $PL_3Ni(CO)_3$ (L = Ph, 2-furyl, 3-furyl) the IR stretching frequencies of the carbonyl groups were measured. The CO stretching frequency depends on the ligand pattern at the phosphorus nuclei, since the electronic properties of the phosphorus substituents are transmitted through the chemical bonds to the carbonyl groups. The carbonyl stretching frequencies extracted from the nickel complexes bearing phosphanes **1a** to **1g** are presented in Table 2.

Both 2-furyl and 3-furyl substituents increase the CO−IR stretching frequency although to different extents. For 2-furyl groups the CO−IR stretching frequency is increased by 3.2 cm^{-1} per additional 2-furyl ligand, and for 3-furyl groups the average increase in CO stretching frequency is only 0.9 cm^{-1}. Increased CO−IR stretching frequencies indicate stronger CO bonds caused by furyl substituents. σ-Donor ligands, which increase the electron density at the phosphorus center, weaken the CO bond, as more electrons can be donated into antibinding π^*-orbitals. The observed increased CO bond strength, however, indicates less electrons in the antibinding π^*-orbitals, thus poor σ-donor capabilities of the furyl bearing phosphanes, which are the result of electron withdrawing properties of the 2-furyl groups. The IR stretching frequency of CO groups in nickel-carbonylphosphanes can be calculated according to Tolman using the formula:[9b]

$$\nu_{CO} = 2056.1 + \sum_{i=1}^{3}\chi_i\ [cm^{-1}] \qquad (1)$$

The value χ_i represents the contribution of every substituent at the phosphorus atom to the overall IR stretching frequency shift. For 2-furyl one can calculate a χ_i value of 7.4 cm^{-1}. Phenyl substituents possess a χ_i value of 4.3 cm^{-1}. 2-Furyl rings are therefore more electron withdrawing to phosphorus atoms than phenyl substituents, for example, ethoxy groups ($\chi_i = 6.8$ cm^{-1}), but less so than methoxy substituents with a χ_i value of 7.7 cm^{-1}. For 3-furyl groups a χ_i value of 5.1 cm^{-1} can be calculated. This is lower than the value of 7.4 cm^{-1} for 2-furyl rings but still electron withdrawing with respect to the phenyl substituent. With respect to Tolmans list of χ_i values,[9b] the 3-furyl system is stronger electron withdrawing than *p*-fluorophenyl substituents with $\chi_i = 5.0$ cm^{-1} and less withdrawing than *p*-chlorophenyl with $\chi_i = 5.6$ cm^{-1}.

From these IR investigations we conclude that 2-furyl and 3-furyl substituents in phosphanes are indeed electron withdrawing in comparison to phenyl rings in triphenylphosphane. Although the electron density on the phosphorus nuclei is reduced, when furyl systems are attached, the phosphorus atoms are shielded. This means that furyl systems cause higher shielded phosphorus nuclei, although less electron density is present. To

---

(11) Strohmeier, W.; Müller, F. J. *Chem. Ber.* **1974**, *96*, 53.
(12) Derencsényi, T. T. *Inorg. Chem.* **1981**, *20*, 665.
(13) Cobley, C. J.; Pringle, P. G. *Inorg. Chim. Acta* **1997**, *265*, 107.
(14) Berners-Price, S. J.; Sadler, P. J. *Structure and Bonding*; Springer-Verlag: Berlin, Heidelberg, 1998; Vol. 70, pp 33−35.
(15) Ikuta, S.; Kebarle, P.; Bancroft, G. M.; Chan, T.; Puddephatt, R. J. *J. Am. Chem. Soc.* **1982**, *104*, 5899.
(16) (a) Schröder, U.; Berger, S. *Eur. J. Org. Chem.* **2000**, 2601. (b) Appel, M.; Berger, S. *Eur. J. Org. Chem.* **2002**, 1143. (c) Ackermann, M.; Berger, S. *Tetrahedron* **2005**, *61*, 6764.

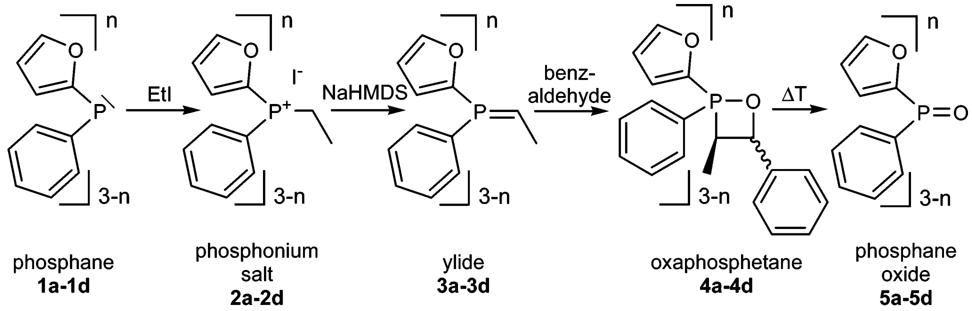

Figure 2. Starting materials, intermediates, and reaction products observed by ^{31}P NMR spectroscopy during Wittig reactions (**a**, triphenyl; **b**−**d**, series of 2-furyl bearing compounds; **e**−**g**, series of 3-furyl systems).

Table 1. ^{31}P NMR Chemical Shift of Intermediates Detected during Wittig Reactions

substituents at phosphorus	δ ^{31}P [ppm] phosphane^a 1	δ ^{31}P [ppm] phosphonium salt^a 2	δ ^{31}P [ppm] ylide^b 3	δ ^{31}P [ppm] oxaphosphetane^{b,c} 4	δ ^{31}P [ppm] phosphane oxide^b 5
Ph_3 **a**	−6.0	26.9	14.8	−60.7^d	24.7
(2-furyl)Ph_2 **b**	−26.3	16.3	2.6	−73.7 (−73.8)	16.4
(2-furyl)$_2$Ph **c**	−50.3	4.4	−12.1	−87.0 (−88.9)	2.3
(2-furyl)$_3$ **d**	−76.8	−9.6	−30.9	−101.4 (−102.0)	−12.9
(3-furyl)Ph_2 **e**	−31.5	17.2	−2.6	−75.7 (−75.8)	20.8
(3-furyl)$_2$Ph **f**	−58.0	7.7	−15.7	−91.1 (−91.2)	12.7
(3-furyl)$_3$ **g**	−82.3	−1.8	−31.2	−103.2 (−103.6)	4.1

[a] ^{31}P NMR chemical shift in $CDCl_3$. [b] ^{31}P NMR chemical shift in [d_8]THF. [c] ^{31}P NMR chemical shift for the *cis*-oxaphosphetane. In parentheses the ^{31}P NMR chemical shift of the *trans*-isomer. [d] Isomers not resolved.

Table 2. IR Stretching Frequencies of Nickelcarbonylphosphane Complexes of the General Formula P(2- or 3-furyl)$_n$Ph$_{3-n}$Ni(CO)$_3$

number *n* of 2-furyl substituents	CO stretching frequency [cm^{-1}]
$n = 0$ (prepared from **1a**)	2068.9
$n = 1$ (prepared from **1b**)	2071.9
$n = 2$ (prepared from **1c**)	2075.4
$n = 3$ (prepared from **1d**)	2078.4
number *n* of 3-furyl substituents	**CO stretching frequency [cm^{-1}]**
$n = 1$ (prepared from **1e**)	2069.8
$n = 2$ (prepared from **1f**)	2070.5
$n = 3$ (prepared from **1g**)	2071.5

solve this apparent contradiction we initiated solid phase MAS NMR studies to have a closer look of the ^{31}P NMR chemical shift tensors.

Solid Phase ^{31}P NMR Investigations

Generally, the shielding of a NMR active nucleus from the outer magnetic field B_0 is generated by electron density around that nucleus. The question arose how electron withdrawing substituents, which decrease the electron density around the phosphorus nucleus, also increase the shielding. To understand the direction in which the ^{31}P NMR chemical shift is moved by different substituents, information on the spatial components of the ^{31}P NMR chemical shift is necessary. Either ^{31}P NMR investigations on oriented single crystals[17] or ^{31}P MAS NMR on polycrystalline powders[18] are suitable to obtain such data. We performed MAS NMR studies on the polycrystalline phosphonium salts **2a**, **2b**, **2c**, and **2d.** Phosphonium salts were chosen for these investigations, since the phosphorus atom lacks the free electron pair. Free electron pairs on phosphorus are known to have multiple influences on the chemical shift, which are difficult to predict and to quantify. 3-Furyl bearing phosphonium salts were not implemented in the ^{31}P MAS NMR[19] investigation, since the overall effects on the chemical shifts were the same as those with 2-furyl groups. The ^{31}P MAS NMR spectra were recorded on a 600 MHz NMR spectrometer (243 MHz for ^{31}P) at room temperature with spinning frequencies of 4000, 3200, 2300, 1400, and 700 Hz. The measurement time varied between 30 min and 5 h, depending on the spinning frequency and the number of spinning sidebands which had to be resolved. As an example, the recorded ^{31}P MAS NMR spectra of ethyltris(2-furyl)phosphonium iodide **2d** at spinning frequencies of 4000 and 700 Hz are shown in Figure 3.

---

(17) (a) Dusold, S.; Maisel, H.; Sebald, A. *J. Magn. Reson*. **1999**, *141*, 78. (b) Ashbrook, S. E.; Wimperis, S. High-resolution NMR of quadrupolar nuclei in solids: The satellite-transition magic angle spinning (STMAS) experiment. *Prog. Nucl. Magn. Reson. Spectrosc.* **2004**, *45*, 53. (c) Kohler, S. J.; Ellett, D. J., Jr.; Klein, M. P. *J. Chem. Phys*. **1976**, *64*, 4451. (d) Kohler, S. J.; Klein, M. P. *Biochemistry* **1976**, *15*, 967. (e) Kohler, S. J.; Klein, M. P. *J. Am. Chem. Soc*. **1977**, *99*, 8290. (f) Herzfeld, G.; Griffin, R. G.; Haberkorn, R. A. *Biochemistry* **1978**, *17*, 2711. (g) Tutunjian, P. N.; Waugh, J. S. *J. Chem. Phys*. **1982**, *76*, 1223. (h) Tutunjian, P. N.; Tropp, J.; Waugh, J. S. *J. Am. Chem. Soc*. **1983**, *105*, 4848. (i) Naito, A.; Sastry, D. L.; McDowell, C. A. *Chem. Phys. Lett*. **1985**, *115*, 19. (j) Hauser, H.; Radloff, C.; Ernst, R. R.; Sundell, S.; Pascher, I. *J. Am. Chem. Soc*. **1988**, *110*, 1054. (k) McDowell, C. A.; Naito, A.; Sastry, D. L.; Takegoshi, K. *J. Magn. Reson*. **1988**, *78*, 498. (l) Ermark, F.; Topic, B.; Haeberlen, U.; Blinc, R. *J. Phys.: Condens. Matter* **1989**, *1*, *5489*. (m) Eichele, K.; Wasylishen, R. E. *J. Phys. Chem*. **1994**, *98*, 3108. (n) Eichele K.; Wu, G.; Wasylishen, R. E.; Britten, J. F. *J. Phys. Chem*. **1995**, *99*, 1030. (o) Lumsden, M. D.; Wasylishen, R. E.; Britten, J. F. *J. Phys. Chem*. **1995**, *99*, 16602. (p) Eichele K.; Wasylishen, R. E.; Maitra, K.; Nelson, J. H.; Britten, J. F. *Inorg. Chem*. **1997**, *36*, 3539. (q) Jensen, T. R.; Hazell, R. G.; Vosegaard, T.; Jakobsen, H. J. *Inorg. Chem*. **2000**, *39*, 2026. (r) Gee, M.; Wasylishen, R. E.; Eichele, K. *J. Phys. Chem. A* **2000**, *104*, 4598. (s) Grossmann, G.; Scheller, D.; Malkina, O. L.; Malkin, V. G.; Zahn, G.; Schmidt, H.; Haeberlen, U. *Solid State Nucl. Magn. Reson*. **2000**, *17*, 22.

(18) (a) Dusold, S.; Klaus, E.; Sebald, A.; Bak, M.; Nielsen, N. C. *J. Am. Chem. Soc*. **1997**, *119*, 7121. (b) Dusold, S.; Milius, W.; Sebald, A. *J. Magn. Reson*. **1998**, *135*, 500. (c) Dusold, S.; Maisel, H.; Sebald, A. *J. Magn. Reson*. **1999**, *141*, 78. (d) Bechmann, M.; Dusold, S.; Forster, H.; Haeberlen, U.; Lis, T.; Sebald, A.; Stumber, M. *Mol. Phys*. **2000**, *98*, 605. (e) Eichele, K.; Wasylishen, R. E.; Corrigan, J. F.; Taylor, N. J.; Carty, A. J.; Feindel, K. W.; Benard, G. M. *J. Am. Chem. Soc*. **2002**, *124*, 1541. (f) Power, W. P.; Wasylishen, R. E. *Inorg. Chem*. **1992**, *31*, 2176. (g) Eichele, K.; Ossenkamp, G. C.; Wasylishen, R. E.; Cameron, T. S. *Inorg. Chem*. **1999**, *38*, 639. (h) Bernard, G. M.; Wu, G.; Lumsden, M. D.; Wasylishen, R. E.; Maigrot, N.; Charrier, C.; Mathey, F. *J. Phys. Chem. A* **1999**, *103*, 1029. (i) Bechmann, M.; Dusold, S.; Geipel, F.; Sebald, A.; Sellmann, D. *J. Phys. Chem. A* **2005**, *109* (24), 5275.

(19) (a) Andrew, E. R.; Bradbury, A.; Eades, R. G. *Nature* **1958**, *182*, 1659. (b) Lowe, I. J. *Phys. Rev. Lett*. **1959**, *2*, 285.

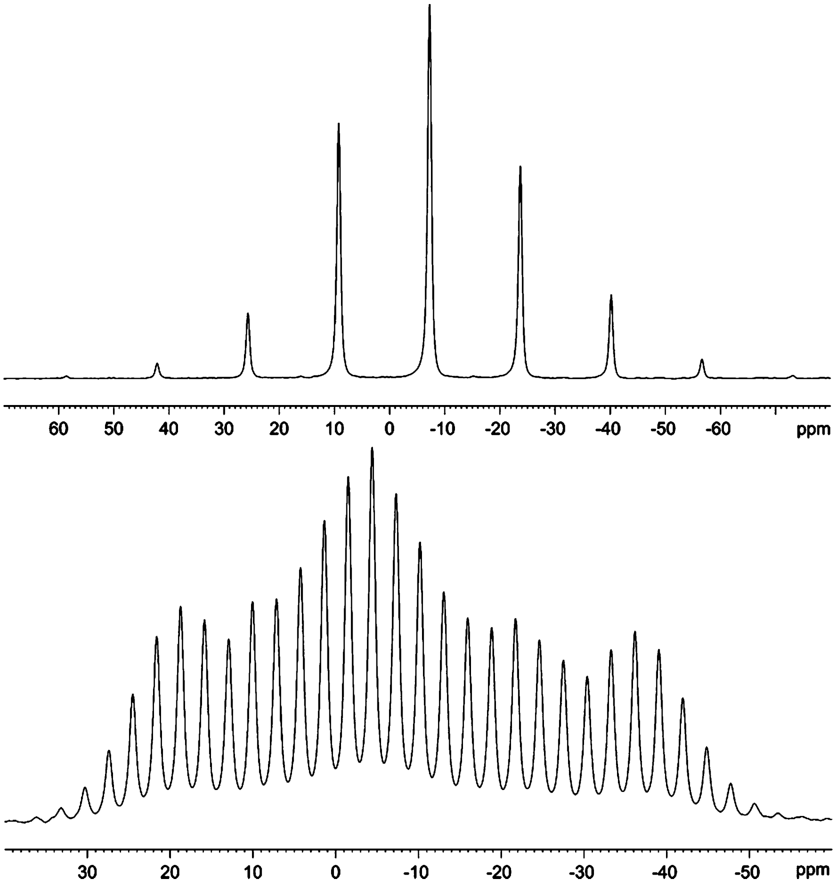

Figure 3. ^{31}P MAS NMR spectra of ethyltris(2-furyl)phosphonium iodide **2d** at MAS frequencies of 4000 Hz (upper picture) and 700 Hz (lower picture).

Table 3. Experimentally Determined Main Axis Chemical Shift Tensor Elements δ_{11}, δ_{22}, δ_{33} for the Four Investigated Phosphonium Salts **2a** to **2d** Together with the Overall Change of the ^{31}P NMR Chemical Shift $\Delta\delta$

phosphonium salt	δ_{iso} [ppm]	δ_{11} [ppm]	δ_{22} [ppm]	δ_{33} [ppm]
$EtP^+Ph_3\ I^-$ **2a**	26.9	42.7	30.9	7.1
$EtP^+Ph_2Fu\ I^-$ **2b**	16.3	39.2	14.7	−5.0
$EtP^+PhFu_2\ I^-$ **2c**	4.4	34.2	14.7	−35.7
$EtP^+Fu_3\ I^-$ **2d**	−9.6	24.8	−5.0	−48.6
$\Delta\delta$	−36.5	−17.9	−35.9	−55.7

It was possible to extract the main axis tensor components of the chemical shift vector δ_{11}, δ_{22}, and δ_{33} from the observed spinning sidebands by a moment analysis known from Maricq and Waugh.[20] The results of these calculations are shown in Table 3.

To visualize the data, these chemical shifts are drawn in Figure 4 versus the number of 2-furyl groups in the phosphonium salts.

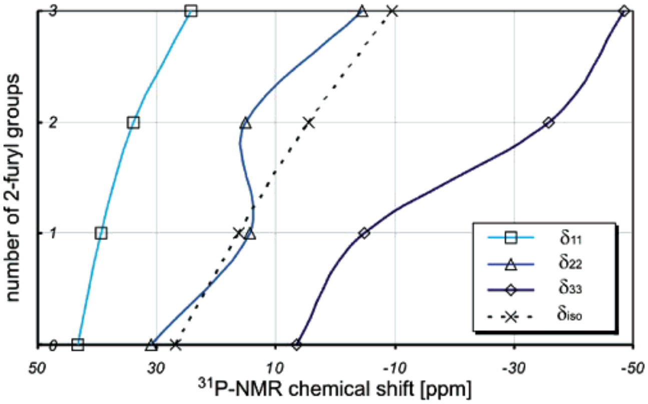

Figure 4. Chemical shift in solution (dotted line) together with the shift of the three main axis components vs the number of 2-furyl groups in the phosphonium salts **2a** to **2d**.

The dotted line in Figure 4 represents the values of the isotropic ^{31}P NMR chemical shift in solution. As discussed above, the isotropic chemical shift for the phosphonium salts in solution is shifted by a total of −36.5 ppm to lower frequencies, if the three phenyl groups in **2a** are replaced by 2-furyl systems leading to **2d**. The three main axis chemical shift tensor elements δ_{11}, δ_{22}, and δ_{33} generally show the same trend to lower resonance frequencies, although to different extents. δ_{11} shows the smallest dependence on the 2-furyl systems and is only shifted by a total of −17.9 ppm to lower frequencies. The strongest influence is visible for δ_{33}, which is shifted by a total of −55.7 ppm to lower frequencies if we compare **2a** with **2d**. We conclude that the chemical shift component δ_{33} provides the main contribution for the significant shift of δ_{iso} to lower resonance frequencies. To understand the unexpected drift of δ_{iso} in solution, we need information on the orientation of δ_{33} within the molecular structure of the phosphonium salts. This question could have been answered if the ^{31}P NMR investigation would have been performed on oriented single crystals. However such information is not accessible with the ^{31}P MAS NMR approach on polycrystalline samples used here. We therefore performed accompanying ab initio quantum chemical calculations of chemical shieldings to clarify why δ_{33} is effected the most in the presence of 2-furyl groups.

---

(20) Maricq, M. M.; Waugh, J. S. *J. Chem. Phys.* **1979**, *70*, 3300.

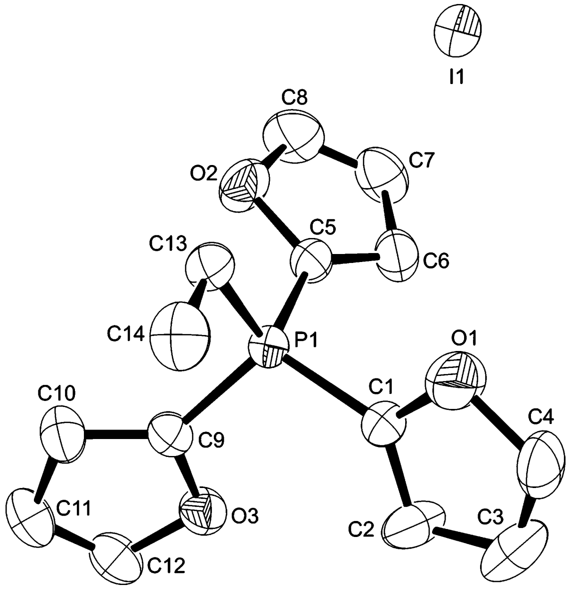

Figure 5. Crystal structure of ethyltris(2-furyl)phosphonium iodide **2d**.

Table 4. Bond Lengths of the Phosphorus−Carbon Bonds in the Crystal Structures. the Average Bond Length Is Given in Cases, in Which More than One Bond of This Type Was Present

phosphonium salt	P–C(ethyl) bond [pm]	P–C(phenyl) bond [pm]	P–C(2-furyl) bond [pm]
$EtP^+Ph_3\ I^-$ **2a**	181.0	179.9	
$EtP^+Ph_2Fu\ I^-$ **2b**	179.4	178.9	176.5
$EtP^+PhFu_2\ I^-$ **2c**	179.6	179.3	176.3
$EtP^+Fu_3\ I^-$ **2d**	178.8		176.6

Theoretical Calculations

For theoretical calculations of the ^{31}P NMR chemical shift tensors we needed the structures of the phosphonium salts in the solid phase. From those structures we should be able to isolate the atomic coordinates, which are required for the ab initio calculations. For this purpose we initiated X-ray crystallographic studies to record the solid phase structures. From the four phosphonium salts under investigation only the ethyltriphenylphosphonium cation X-ray structure is known. For our studies we used the X-ray structure of ethyltriphenylphosphonium triiodide,[21] since the difference in the cation structure whether iodide or triiodide is present as anion should be small. This compound crystallizes in a monoclinic crystal system with the space group *P*2(1)/*n*. The crystal structures of 2-furyl bearing phosphonium salts **2b** to **2d** have not been published in the literature and therefore had to be determined. The crystals were grown in a solution of ethanol with ethyl acetate at a temperature of −27 °C. In Figure 5 the structure of ethyltris(2-furyl)phosphonium iodide **2d** is shown. The crystal structures of **2b** and **2c** are given in the Supporting Information.

This molecule crystallizes in a monoclinic crystal system with the space group *P*2(1)/*c*. If one compares the bond lengths of the phosphorus−carbon(substituent) bonds in the crystal structures of the cations in **2a** to **2d** an interesting trend is revealed. The average bond lengths in the investigated crystal structures are shown in Table 4.

The bond length of the phosphorus−carbon(ethyl) bond decreases as the number of 2-furyl groups present in the molecule increases. Furthermore, the P−C(substituent) bonds become longer by an average of 2.7 pm, when 2-furyl groups instead of phenyl rings are attached to the phosphorus. This is an indication, that under the presence of 2-furyl groups the orbital overlap is better, leading to shorter bonds and presumably more stable molecules.

Table 5. Calculated Absolute Shieldings $\sigma(S)_g$ for the Phosphorus Atoms in the Four Phosphonium Cations of **2a**−**2d** and for the Chloride Salt of **2d**, with the Corresponding Calculated Relative ^{31}P NMR Chemical Shifts $\delta(S)_g$ in the Gas Phase and the Experimental ^{31}P NMR Chemical Shifts for the Iodide Salts of **2a**−**2d** in the Liquid Phase in $CDCl_3$[a]

		basis set			
		6-311G(d,p)	TZ2P	G3large	expmt
EtP^+Ph_3 **2a**	$\sigma(S)_g$ [ppm]	287.6	299.3	265.9	
	$\delta(S)_g$ [ppm]	40.8	29.0	62.4	26.9
EtP^+Ph_2Fu **2b**	$\sigma(S)_g$ [ppm]	303.5	314.3	280.8	
	$\delta(S)_g$ [ppm]	24.9	14.1	47.6	16.3
EtP^+PhFu_2 **2c**	$\sigma(S)_g$ [ppm]	320.5	331.2	294.8	
	$\delta(S)_g$ [ppm]	7.8	−2.9	33.6	4.4
EtP^+Fu_3 **2d**	$\sigma(S)_g$ [ppm]	332.5	341.1	309.1	
	$\delta(S)_g$ [ppm]	−4.1	−12.7	19.3	−9.6
$EtP^+Fu_3\ Cl^-$	$\sigma(S)_g$ [ppm]	329.4	337.4	306.1	
	$\delta(S)_g$ [ppm]	−1.1	−9.1	22.2	

[a] $\sigma(S)_g$ values calculated with 6-311G(d,p), (TZ2P),[22c] and [G3large][22d] basis sets, respectively

Calculations of magnetic shieldings were performed using the Gaussian program suite.[22] We used the B3LYP hybrid density functional method to describe the N-electron space.[22b] The one-electron space was explored using different basis set models, the standard 6-311G(d,p) basis set, a TZ2P[22c] basis set, and the G3large basis set used in G3 theory. The relative calculation times on dual CPU Opteron 248 workstations were 1: 5: 28.

The atomic coordinates from the crystal structures were used to generate the geometries for the input of the NMR calculations. We calculated the magnetic shieldings for the isolated cation structures **2a**−**2d** without the iodide anion. Comparative calculations performed for the salt **2d** where the iodide anion was substituted by a chloride anion revealed that the anion exhibits negligible influence on absolute isotropic shielding of the phosphorus atom (around −3 ppm, see Table 5). The absolute shieldings were transformed into chemical shifts referenced to aqueous H_3PO_4 using the equation:[23]

$$\delta(S) = \sigma(H_3PO_4) - \sigma(S) \text{ with } \sigma(H_3PO_4) = 328.35 \text{ ppm} \quad (2)$$

Table 5 shows the calculated absolute isotropic shieldings and the relative chemical shifts according to eq 2 for the isolated phosphonium cations **2a**−**2d** without anion and for the salt **2d** with chloride as anion.

The calculated absolute shieldings are highly dependent on the basis set employed (Table 5). The gas-phase isotropic ^{31}P NMR chemical shifts $\delta(S)_g$ calculated using b3lyp/6-311g(d,p) deviate by an average of 7.8 ppm from the experimental chemical shift in solution. The data obtained with the TZ2P basis set are in reasonable agreement and deviate only by 3.7 ppm in the average, whereas the data from the G3large basis set are off by 31.2 ppm in the average. The differences are in part due to the model used to describe the one electron space. Basis sets are optimized for modeling valence electrons better than core electrons, whereas NMR experiments also probe the electron density closer to the nuclei. Discrepancies between experimental chemical shifts in solution and the calculated data are also expected

---

(21) Tebbe, K.-F.; Farida, T. Z. *Naturforsch*. **1995**, *50b*, 1685.

(22) (a) Gaussian 03, Revision D.01/D02, Frisch, M. J. et al. *Gaussian, Inc*, Wallingford CT, 2004. For full citation, see Supporting Information. (b) Becke, A. D. *J. Chem. Phys*. **1993**, *98*, 5648. (c) The TZ2P basis set was constructed from the Dunning triple-ζ set (Dunning, T. H., Jr. *J. Chem. Phys*. **1971**, *55*, 716. available from http://www.emsl.pnl.gov/forms/basisform.html. For phosphorus and chlorine the 6s5p contraction of the Huzinaga 12s9p scheme was used as reported in McLean, A. D.; Chandler, G. S. *J. Chem. Phys*. **1980**, *72* (10), 5639. The standard pairs of polarization function were added by C. Janssen April 5, 1991 as suggested by Brian Yates, see: http://zopyros.ccqc.uga.edu/psi/Psiman/basis_set_info.txt. (d) The G3large basis set corresponds to the G3large basis set used in the MP2(full) calculation in G3 theory (Curtiss, L. A.; Raghavachari, K.; Redfern, P. C.; Rassolov, V.; Pople, J. A. *J. Chem. Phys*. **1998**, *109*, 7764). See: http://chemistry.anl.gov/compmat/G3basis/hkrg3l.txt

(23) Jameson, C. J.; de Dios, A.; Jameson, A. K. *Chem. Phys. Lett*. **1990**, *167*, 575.

Table 6. Calculated (B3LYP/TZ2P) Main Axis Components of the Chemical Shift Tensor in the Gas Phase $\delta_{11,g}$, $\delta_{22,g}$, $\delta_{33,g}$ Together with the Experimental Values $\delta_{11,s}$ to $\delta_{33,s}$ Determined by ^{31}P MAS NMR from Table 3

	$\delta_{11,g}$ [ppm]	$\delta_{11,s}$ [ppm]	$\delta_{22,g}$ [ppm]	$\delta_{22,s}$ [ppm]	$\delta_{33,g}$ [ppm]	$\delta_{33,s}$ [ppm]
EtP^+Ph_3 **2a**	38.6	42.7	30.7	30.9	17.7	7.1
EtP^+Ph_2Fu **2b**	37.0	39.2	9.3	14.7	−4.1	−5.0
EtP^+PhFu_2 **2c**	26.6	34.2	7.2	14.7	−42.5	−35.7
EtP^+Fu_3 **2d**	18.4	24.8	−10.5	−5.0	−46.0	−48.6
$EtP^+Fu_3\ Cl^-$	24.1		−4.7		−46.6	

because solute−solvent interactions are not considered in the model calculations. Despite these shortcomings of the calculation model, it is of utmost importance for the context of these investigations that the calculations with all three basis sets are very consistent by predicting 10 to 16 ppm higher shielding for each added furyl ring. The experimental result that the resonance frequencies in solution are shifted to lower frequencies when phenyl substituents are replaced by 2-furyl groups is confirmed by the calculated gas-phase chemical shifts.

We have further calculated the main axis components of the ^{31}P NMR chemical shift in the gas phase. Table 6 shows a comparison of the calculated values (B3LYP/TZ2P) of the main axis components of the ^{31}P NMR chemical shift tensor with the experimentally determined values. The individual tensor values obtained for the 6-311G(d,p) and G3large basis sets are very similar and show consistency. They are given in the Supporting Information.

The similarities between the experimental results and the quantum chemical calculations are striking. The three main axis components of the ^{31}P NMR chemical shift are shifted to lower resonance frequencies under the influence of 2-furyl substituents. Consistent with the experimental results the calculated tensor component δ_{33} shows the largest effect. The shielding difference of δ_{33} going from compound **2a** to **2d** is 63.6 ppm according to the calculations and 55.7 ppm from experimental results. Of highest interest is the orientation of this component within the molecular geometry. This information is available from the eigenvector also calculated by Gaussian.

The calculated orientation of the main axis shielding tensor components within the molecule is shown in Figure 6 for the ethyltris(2-furyl)phosphonium cation **2d**. Results for the compounds **2a** to **2c** are given in the Supporting Information.

The main attention should be drawn to the component σ_{33}, the shielding value of the chemical shift component δ_{33}, which was identified above as the most sensitive tensor component. σ_{33} is almost parallel to the *z*-axis of the molecule coordinate system, with an angle between the *z*-axis and σ_{33} of 7.2°. The angular difference between the direction of the P−C(ethyl) bond and the component σ_{33} is even lower (5.2°). Comparable orientations for the component σ_{33} and the P−C(ethyl) bond could be observed in every compound investigated. The angles between these two vectors were 39.3° in the cation of **2a**, 37.8° in **2b**, and 23.9° in **2c** as calculated with the tz2p basis set. The angles observed with the other employed basis sets are very similar. These results verify that the most sensitive shielding component σ_{33} is oriented almost parallel to the P−C(ethyl) bond and therefore at the same time almost perpendicular to the P−C(substituent) bonds in the four phosphonium salt structures. As a consequence σ_{33} is most sensitive concerning changes in the electron density of the P−C(substituent) bonds.

At this point, the main axis shielding component σ_{33} has been identified as the most sensitive shielding component, and it could be rationalized that this sensitivity has its origin in the orientation of that component σ_{33} within the molecule. Still unclear is why are all components shifted to lower resonance frequencies, meaning that the phosphorus nucleus gets better shielded from the outer magnetic field.

This question might be answered when taking into account that the P−C(phenyl) bonds are longer than P−C(2-furyl) bonds (Table 4). A shorter bond length can be attributed to better orbital overlap and finally more stable molecules, with a lower ground state energy. A lower ground state energy leads generally to higher activation energies Δ*E*. According to the Pople equation:[24]

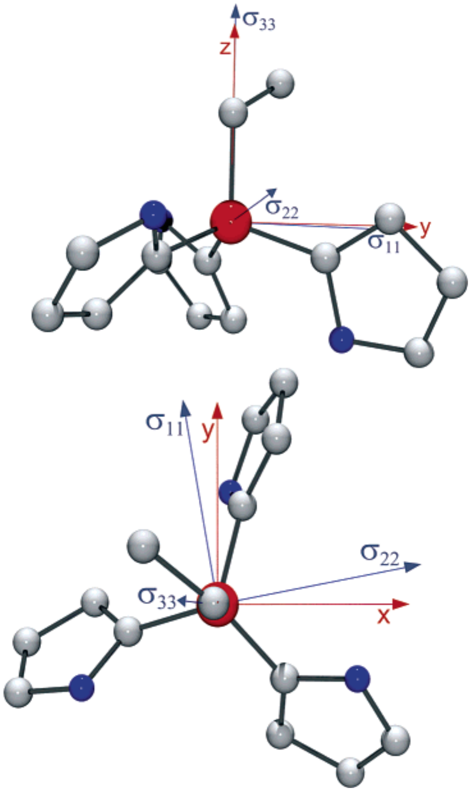

Figure 6. Orientation of the main axis shielding components within the crystal structure of ethyltris(2-furyl)phosphonium cation as calculated with the tz2p basis set. **2d**. Bottom: View in direction of the negative *z*-axis of the molecule coordinate system. Top: View in direction of the negative *x*-axis.

$$\sigma^{\mathrm{para}}_{\mathrm{iso}} = -\frac{\mu_0\mu_B^2}{2\pi\Delta E}\langle r^{-3}\rangle\left[Q_i + \sum_{i\neq j} Q_j\right] \qquad (3)$$

Δ*E* is inversely proportional to σ^{para}, which is one component of the overall magnetic shielding of any nucleus given by eq 4:

$$\sigma_{\mathrm{iso}} = \sigma^{\mathrm{dia}}_{\mathrm{iso}} + \sigma^{\mathrm{para}}_{\mathrm{iso}} + \sum_{i\neq j}\sigma_j \qquad (4)$$

The component σ^{iso} arises from core near s-electrons and always increases the overall shielding, whereas σ^{para} has its origin in the p-electron density and always acts as a deshielding influence. According to the Pople equation, a higher activation energy Δ*E* results in a decreased σ^{para} term. Due to the deshielding influence of the σ^{para} term, the final concequence is an increase in the overall shielding of the nucleus of interest. This explains why the exchange of phenyl ligands by more electron withdrawing 2-furyl groups leads to lower ^{31}P NMR resonance frequencies. Electron density is withdrawn from the p-electrons, the influence of the deshielding σ^{para} term is reduced, leading to a higher overall shielding of the phosphorus nuclei, which results in a significant shift of all ^{31}P NMR resonances to lower frequencies under the presence of 2-furyl groups.

Conclusion

In this work the electronic influences of 2- and 3-furyl substituents at phosphorus atoms on the ^{31}P NMR chemical shift

---

(24) Karplus, M.; Pople, J. A. *J. Chem. Phys.* **1963**, *38*, 2803.

were studied. An extensive shift of ^{31}P NMR resonances to lower frequencies is observed, when phenyl groups attached to phosphorus are replaced by 2-furyl or 3-furyl rings indicating an increased overall shielding of phosphorus nuclei under these conditions. IR investigations confirmed that 2- and 3-furyl substituents act electron withdrawing on phosphorus nuclei with respect to standard phenyl rings. The question arose why the shielding of phosphorus atoms under the presence of furyl systems is increased, although the electron density is reduced by these furyl systems. The principal chemical shift tensor components were extracted from solid state ^{31}P MAS NMR spectra, showing that all three components are shifted to lower NMR frequencies, but the component δ_{33} to the largest extent. The orientation of this shift component within the molecules was calculated using ab initio methods. δ_{33} stands almost perpendicular to the P−C(phenyl or furyl) bonds in the investigated molecules, proving the reason for the observed shift of NMR resonances has its origin in changed electronic properties of the P−C(furyl) bonds. Furthermore, X-ray crystallography studies showed that P−C(furyl) bonds are significantly shorter than the bonds to phenyl groups. This indicates better orbital overlap, leading to lower ground-state energies of molecules containing 2-furyl groups. These facts result in an increased activation energy of the phosphonium salts, which lowers the deshielding contribution of the σ^{para} term to the overall magnetic shielding. We therefore observe an increased overall magnetic shielding of the ^{31}P nuclei under the presence of 2-furyl groups, bringing this trend in harmony with the electron withdrawing properties of the furyl substituents.

Experimental Section

NMR Investigations: ^{31}P NMR spectra in liquids and all spectra measured at low temperatures were recorded on a BRUKER DRX-400 spectrometer in either $CDCl_3$ or [d_8]THF as solvent. The solid phase ^{31}P MAS NMR spectra were recorded on a BRUKER DRX-600 with a CP/MAS NMR Probe DOTY DSI 750.

IR Investigations: IR spectra were recorded on an Avatar 360 FT-IR ESR spectrometer from THERMO NICOLET. The nickelcarbonylphosphane complexes were prepared by shaking a 0.2 M $Ni(CO)_4$ solution in CH_2Cl_2 with a 0.2 M phosphane solution in CH_2Cl_2 at room temperature. The solution was directly measured as film between KBr plates.

X-ray Crystallography: Suitable crystals for crystal structure analysis were obtained by carefully recrystallizing the solids in a mixture of ethanol and ethyl acetate. The crystals were grown for several days at a temperature of −27 °C. A CCD X-ray diffractometer from BRUKER was used to determine the crystal structures. The structures were recorded at 220 K. Ethyl(2-furyl)-diphenylphosphonium iodide ($C_{18}H_{18}IOP$, 408,2 g/mol) grew in a triclinic unit cell with the space group $P\bar{1}$. Ethylbis(2-furyl)-phenylphosphonium iodide ($C_{16}H_{16}IO_2P$, 398,18 g/mol) had an orthorhombic unit cell with the space group *Pca*2 (1). Ethyltris-(2-furyl)phosphonium iodide ($C_{14}H_{14}IO_3P$, 388.14 g/mol) grew in a monoclinic crystal system with the space group *P*2(1)/*c*.

Quantum chemical calculations were performed at Ulm university using the Gaussian program suite[22] on a SUSE LINUX AMD Athlon and Opteron cluster.

Acknowledgment. We thank the Verband der Chemischen Industrie for a Chemiefonds-Stipendium Grant Number 168291 (University of Leipzig) and for financial support for computer equipment (University of Ulm). Furthermore we thank Prof. Dr. W. Petz (Marburg) for the generous support with $Ni(CO)_4$. We thank Prof. Dr. H. Krautscheid (Leipzig) and Dr. K. Eichele (Tübingen) for very helpful discussions.

Supporting Information Available: Detailed moment analysis; crystal structures of ethyl(2-furyl)diphenylphosphonium iodide **2b** and ethylbis(2-furyl)phenylphosphonium iodide **2c**; cif files for the crystal structures of **2b**, **2c**, and **2d**; graphical representations for the main axis shielding components and their orientation within the molecules **2a**, **2b**, and **2c**; chemical shift tensor values obtained for the 6-311G(d,p) and G3large basis sets. This material is available free of charge via the Internet at http://pubs.acs.org.

JA057085U